Development 134, 3327-3338 (2007) doi:10.1242/dev.007674

SULF1 and SULF2 regulate heparan sulfate-mediated GDNF signaling for esophageal innervation

Xingbin Ai[1,*], Toshio Kitazawa[1], Anh-Tri Do[2], Marion Kusche-Gullberg[3], Patricia A. Labosky[4] and Charles P. Emerson, Jr[1,*]

Heparan sulfate (HS) plays an essential role in extracellular signaling during development. Biochemical studies have established that HS binding to ligands and receptors is regulated by the fine 6-O-sulfated structure of HS; however, mechanisms that control sulfated HS structure and associated signaling functions in vivo are not known. Extracellular HS 6-O-endosulfatases, SULF1 and SULF2, are candidate enzymatic regulators of HS 6-O-sulfated structure and modulate HS-dependent signaling. To investigate Sulf regulation of developmental signaling, we have disrupted Sulf genes in mouse and identified redundant functions of Sulfs in GDNF-dependent neural innervation and enteric glial formation in the esophagus, resulting in esophageal contractile malfunction in *Sulf1*$^{-/-}$;*Sulf2*$^{-/-}$ mice. SULF1 is expressed in GDNF-expressing esophageal muscle and SULF2 in innervating neurons, establishing their direct functions in esophageal innervation. Biochemical and cell signaling studies show that Sulfs are the major regulators of HS 6-O-desulfation, acting to reduce GDNF binding to HS and to enhance GDNF signaling and neurite sprouting in the embryonic esophagus. The functional specificity of Sulfs in GDNF signaling during esophageal innervation was established by showing that the neurite sprouting is selectively dependent on GDNF, but not on neurotrophins or other signaling ligands. These findings provide the first in vivo evidence that Sulfs are essential developmental regulators of cellular HS 6-O-sulfation for matrix transmission and reception of GDNF signal from muscle to innervating neurons.

KEY WORDS: SULF1, SULF2, Heparan sulfate, GDNF, Esophagus, Innervation, Intrinsic neuron, Enteric glial cell, Neural crest progenitor, Mouse

INTRODUCTION

Heparan sulfate (HS) regulates a number of extracellular signaling pathways that are essential for embryonic development (Lin, 2004). HS is a linear polysaccharide chain covalently attached to a protein core of heparan sulfate proteoglycans (HSPGs) and consists of repeating disaccharide units of uronic acid linked to glucosamine (Esko and Lindahl, 2001). During HS biosynthesis in the Golgi, disaccharide units can be sulfated at the 2-O position of uronic acid and N-, 3-O and 6-O positions of glucosamine by specific sulfotransferases. Sulfation along the HS chain is incomplete, thus creating highly sulfated domains separated by partially sulfated and non-sulfated domains. The highly sulfated domain interacts with a variety of extracellular signaling ligands and receptors and is therefore considered the major signaling domain of HS. However, owing to a lack of biochemical tools and genetic models through which specific sulfate groups of HS can be modified, it remains controversial whether such interactions are determined non-selectively by the overall negative charge, or selectively through establishment of fine sulfated HS sequences – an 'HS code'– within the highly sulfated domain (Kreuger et al., 2006).

Sulfs are newly discovered extracellular heparan sulfate 6-O-endosulfatases that have unique structural features, enzymatic activities and signaling functions (Ai et al., 2005). Sulfs contain the essential enzymatic sequences conserved among all sulfatases, as well as distinct hydrophilic sequences that are required both to dock Sulfs on the cell surface and for their enzymatic activities (Dhoot et al., 2001; Ai et al., 2006). SULF1 and SULF2 in vertebrates have similar substrate specificity towards a selective subset of 6-O-sulfate groups within the highly sulfated domain of HS chains, implicating these enzymes as regulators of the 'HS code' (Morimoto-Tomita et al., 2002; Ai et al., 2003). Sulfs remodel HS 6-O-sulfation pattern on the cell surface to regulate HS binding to signal ligands and receptors in a diversity of signaling pathways, including Wnt, FGF and HGF, BMP and SHH (Ai et al., 2005). Sulfs are dynamically expressed in the embryonic tissues (Dhoot et al., 2001; Danesin et al., 2006; Lum et al., 2007). Avian SULF1 controls Wnt-dependent myogenic specification and is implicated in SHH-regulated oligodendroglial specification (Dhoot et al., 2001; Danesin et al., 2006).

The functions of Sulfs in mammals are unknown. Recent studies report that Sulf single- and double-mutant mice appear normal at birth, and *Sulf2*$^{-/-}$ and *Sulf1*$^{-/-}$;*Sulf2*$^{-/-}$ mice have reduced body weight and double-mutant mice die soon after birth (Lum et al., 2007; Lamanna et al., 2006), although the cellular basis for this growth phenotype was not identified. To investigate the developmental signaling functions of Sulfs, we established independent lines of Sulf mutant mice using gene targeting. We identify a primary neuronal innervation defect of *Sulf1*$^{-/-}$;*Sulf2*$^{-/-}$ esophagi, providing an explanation for the severe growth defects in these mice. Furthermore, we show that this esophageal defect in *Sulf1*$^{-/-}$;*Sulf2*$^{-/-}$ mice is due to aberrant GDNF signaling.

The neuronal innervation of muscles along the gastrointestinal tract is controlled by GDNF, a HS-dependent neurotrophic factor derived from the target muscles (Baloh, et al., 2000; Barnett et al., 2002; Rickard et al., 2003). In the embryonic esophagi, muscle progenitors express GDNF beginning at embryonic day (E) 10, peaking between E11 and E16 and diminishing at E18 (Golden et al., 1999). GDNF not only promotes the proliferation of the enteric

[1]Boston Biomedical Research Institute, Watertown, MA 02472, USA. [2]Department of Medical Biochemistry and Microbiology, Uppsala University Biomedical Center, PO Box 582, S-75123, Uppsala, Sweden. [3]Department of Biomedicine, Division of Physiology, University of Bergen, Jonas Lies vei 91, 5009 Bergen, Norway. [4]Center for Stem Cell Biology, Vanderbilt University, Nashville, TN 37232, USA.

*Authors for correspondence (e-mails: xingbina@bbri.org; emersonc@bbri.org)

Accepted 14 July 2007

neural crest precursors and support their neuronal and glial differentiation (Heuckeroth et al., 1998), but also acts as a target-derived chemoattractant for directed neurite outgrowth of both 'intrinsic' enteric neurons and 'extrinsic' neurons whose cell bodies are located in ganglia outside of the esophagus (Young et al., 2001; Yan et al., 2004). Neurons reach the target muscle during the initiation of GDNF expression in the embryonic esophagus (Durbec et al., 1996; Sang and Young, 1997), and the formation of functional innervations and enteric glial cells initiates in the embryo and proceeds postnatally until completion around two weeks after birth (Sang and Young, 1997; Breuer et al., 2004). The esophageal muscle in the muscularis externa (ME) matures from smooth muscle to skeletal muscle along with the neuronal innervation (Rishniw et al., 2003). In the adult esophagi, the striated muscle in the ME is innervated by both intrinsic and extrinsic neurons (Sang and Young, 1998; Neuhuber et al., 2006), whereas the smooth muscle in the muscularis mucosae is directly innervated mostly by intrinsic neurons, which elicit the smooth muscle contractility in response to extrinsic nerves, as suggested by previous electrophysiological studies (Kamikawa and Shimo, 1979; Storr et al., 2001; Worl et al., 2002). Defects in neural innervation can lead to neonatal death and a variety of esophageal disorders, such as achalasia and a motility disorder, congenital idiopathic megaesophagus (Longstretch and Walker, 1994; Neuhuber et al., 2006).

GDNF signaling requires 2-O- and 6-O-sulfate groups of HS or heparin, a highly sulfated HS derivative, for binding to HS and for GDNF signaling (Barnett et al., 2002; Rickard et al., 2003). Whether Sulfs regulate the GDNF signaling pathway has not been investigated. In this study, we establish that Sulfs are required for GDNF signaling during esophageal innervation. We show that Sulf mutant HS has a highly selective increase of the trisulfated disaccharides without affecting other structural properties, establishing Sulfs as major regulators of cellular HS 6-O-desulfation. Furthermore, SULF1 and SULF2 are dynamically and differentially expressed by the GDNF-expressing muscle progenitors and neuronal progenitors to promote GDNF-mediated neurite sprouting. By further demonstrating that neurite outgrowth of the esophageal explants requires GDNF, but not neurotrophins or other previously known Sulf-regulated signaling ligands, we establish functional specificity of Sulfs in the GDNF pathway during esophageal innervation. Our findings provide the first evidence that Sulf enzymes are in vivo regulators of an 'HS code' that controls HS fine sulfated structures to coordinate the responses of Sulf-expressing cells to developmental signals.

MATERIALS AND METHODS

Mice

Sulf mutant mice were generated as described (see Figs S1, S2 in the supplementary material) (Tompers and Labosky, 2004). Genotyping was performed by DNA extraction from tail followed by PCR. The Sulf single-mutant mice, maintained as heterozygous, were backcrossed into C57BL6 background (sixth generation). The *Sulf1*$^{-/-}$ and *Sulf2*$^{-/-}$ mice were mated to generate the double-heterozygous mutants. *Sulf1*$^{-/-}$;*Sulf2*$^{-/-}$ mice or embryos were generated by crossing *Sulf1*$^{+/-}$;*Sulf2*$^{+/-}$ mice with *Sulf1*$^{-/-}$;*Sulf2*$^{+/-}$ mice or by mating between *Sulf1*$^{-/-}$;*Sulf2*$^{+/-}$ mice. The *Sulf1*$^{-/-}$;*Sulf2*$^{-/-}$ mice were in a mixed 129SvEv/C57BL/6 genetic background.

Histochemistry

The lower-half thoracic segment of the esophagus was dissected from control and *Sulf1*$^{-/-}$;*Sulf2*$^{-/-}$ mice, rinsed gently in ice-cold PBS and fixed in periodate-lysine-paraformaldehyde (PLP) for 2 hours at 4°C. Tissues were then embedded in OCT and 10 μm serial cryosections were collected. Sections were stained with Hematoxylin and Eosin (H&E). Adjacent, unstained sections were used for immunohistochemical studies (see below).

Single- and multi-label immunohistochemistry

Immunohistochemistry on tissue sections was performed as described previously (Ai et al., 2003), except for an additional 1-hour blocking with MOM blocking reagent (Vector) for mouse monoclonal antibodies. Antigen-antibody complexes were detected either by fluorescence or by chromogenic substrate. For explant cultures or whole-mount staining, the washes were extended to 30 minutes each. Primary antibodies included: (1) rabbit anti-glial fibrillary acidic protein (GFAP) (Dako; 1:100); (2) rabbit anti-MS1HD (1:100); (3) rabbit anti-MS2HD (1:100); (4) mouse anti-skeletal fast myosin (clone MY-32) alkaline phosphatase conjugate (Sigma; 1:300); (5) goat anti-GDNF (R&D Systems; 2 μg/ml); (6) mouse anti-neuron-specific class III β-tubulin antibody (clone TuJ1) (R&D Systems; 1:500); (7) rabbit anti-smooth muscle-specific SM22 (a gift from Dr Mario Gimona, Austrian Academy of Sciences; 1:1000); (8) rabbit anti-p75 (Upstate; 1:200); (9) goat anti-GFRα1 (R&D systems; 1 μg/ml); (10) rabbit anti-RET (Santa Cruz Biotechnology; 1:50); (11) rabbit anti-phosphorylated p44/42 MAPK (Cell Signaling; 1:500).

Esophagus explant cultures

The ~400 μm esophagus was dissected from E11.5 mouse embryos and cultured in 500 μl growth medium (DMEM plus 10% fetal bovine serum; Mediatech) on presolidified collagen gel in a 24-well plate. GDNF, NGF, BDNF, NT3 or NT4 (R&D Systems) were added immediately to the collagen/DMEM mixture at various concentrations. Esophagus explants were cultured on collagen gel for 4-5 days before fixation with 4% paraformaldehyde in PBS followed by immunohistochemistry as described above. After antigen-antibody complexes were detected by diaminobenzine (DAB) substrate, the explants were examined using a Nikon TS100 microscope and photographed using a Nikon E4300 camera to show the whole explant with extended neuritis. To quantify the number of neurons in the explant, immunostained explants were examined using a Leica DMR microscope and photographed using a Leica DC300F camera.

Tissue culture

Cells were cultured in growth medium plus 1% antibiotics (Gibco). To activate signaling, cells (1×10^5 per well of a 24-well plate) were serum-starved in DMEM for 6 hours before adding GDNF or NGF at various concentrations. After stimulation, cells were lysed for western blot or for co-immunoprecipitation.

Immunoblot analysis

Immunoblot analysis was as described previously (Dhoot et al., 2001). The intensity of the signal was quantified by Multi-analysis software (Bio-Rad). The primary antibodies for immunoblots included: rabbit anti-MAPK (1:4000; Sigma), mouse anti-phosphorylated MAPK (1:1000; Sigma), rabbit anti-phosphorylated AKT (1:1000; Cell Signaling), rabbit anti-GDNF (0.5 μg/ml); mouse anti-phosphorylated Tyr (1:1000; Calbiochem); rabbit anti-RET (1:500).

Measurement of contraction forces of the esophagus skeletal muscle and smooth muscle

Esophagus was dissected from P12 or adult mice. To measure contractions of skeletal muscles, the 5-mm longitudinal esophagus slices were cut out, tied with silk threads at both ends and hooked up to tungsten needle tips. One of the needles was connected to a force transducer (AM801, SensoNor, Horten, Norway) and the other to a micromanipulator to stretch the muscle length to 1.1 times the slack. Platinum electrode wires were placed near the tubes on both sides. The esophagus slices were stimulated by 1-millisecond duration square pulses (TSS20, Intracel, UK), one single pulse for twitch and 30 Hz for 1 minute for tetanus. To measure contractions of smooth muscle, the smooth muscle cross-rings were dissected from 1-mm esophagus tubes and then hooked up to two needle tips. The rings were stretched to 1.2-1.3 times the slack. The muscle preparations were then immersed into the normal external solution [150 mM NaCl, 4 mM KCl, 2 mM Ca-methanesulphonate (Ca-Ms), 2 mM Mg-Ms, 5.6 mM glucose, 5 mM N-2-hydroxyethylpiperazine-N′-2-ethanesulfonic acid, pH 7.4] in a well on a bubble plate to allow for rapid solution exchange. Force records were amplified with a bridge-amplifier, which was connected to a data-acquisition system (PowerLab, ADInstruments, Colorado Spring, CO).

Depolarizing external solution had K-Ms substituted equally for NaCl with other chemicals in the same concentrations. Compounds used in the recoding were applied at the following final concentrations: 10 μM atropine, 2 μg/ml alpha-BTx, 100 μM ATP, 124 mM K^+, 30 μM histamine and 30 μM carbachol. All experiments were carried out at 30°C.

GDNF binding to heparin and GFRα1

SULF1 digestion of heparin or heparin-conjugated agarose beads (Sigma) was performed as described previously (Ai et al., 2006). To allow GDNF binding to heparin, 20 μl of digested heparin-conjugated agarose beads were incubated with GDNF in PBS (a total volume of 100 μl) at room temperature for 1 hour. The amount of GDNF bound to the heparin-conjugated agarose beads was assayed by immunoblot analysis. To allow GDNF binding to GFRα1, 10 ng GDNF, 1 μg GFRα1-Fc and heparin were mixed in 50 μl PBS for 30 minutes at room temperature. The GDNF-heparin-GFRα1-Fc complex was purified with 10 μl protein A-agarose beads. The amount of GDNF bound to GFRα1 was assayed by immunoblot analysis.

HS preparation and disaccharide analysis

Mouse embryonic fibroblasts (MEFs) were isolated from the skin of E14.5 mouse embryos after dissociation with dispase II (Boehringer Mannheim; 2 mg/ml). MEFs were cultured in DMEM with 10% fetal bovine serum. The radiolabeling, preparation and structural analysis of the HS were performed as described previously (Ai et al., 2003).

RESULTS

Sulf1$^{-/-}$;*Sulf2*$^{-/-}$ mice have abnormal HS sulfation, postnatal growth defects and enlarged esophagi

To investigate Sulf regulation of developmental signaling, we generated mice with targeted deletions of the second coding exon (exon 2) of *Sulf1* and *Sulf2* using Cre-loxP technology (see Figs S1, S2 in the supplementary material). Exon 2 encodes essential amino acids in the enzymatic domains of SULF1 and SULF2 (Dhoot et al., 2001). Although Sulf mutant embryos express partial Sulf

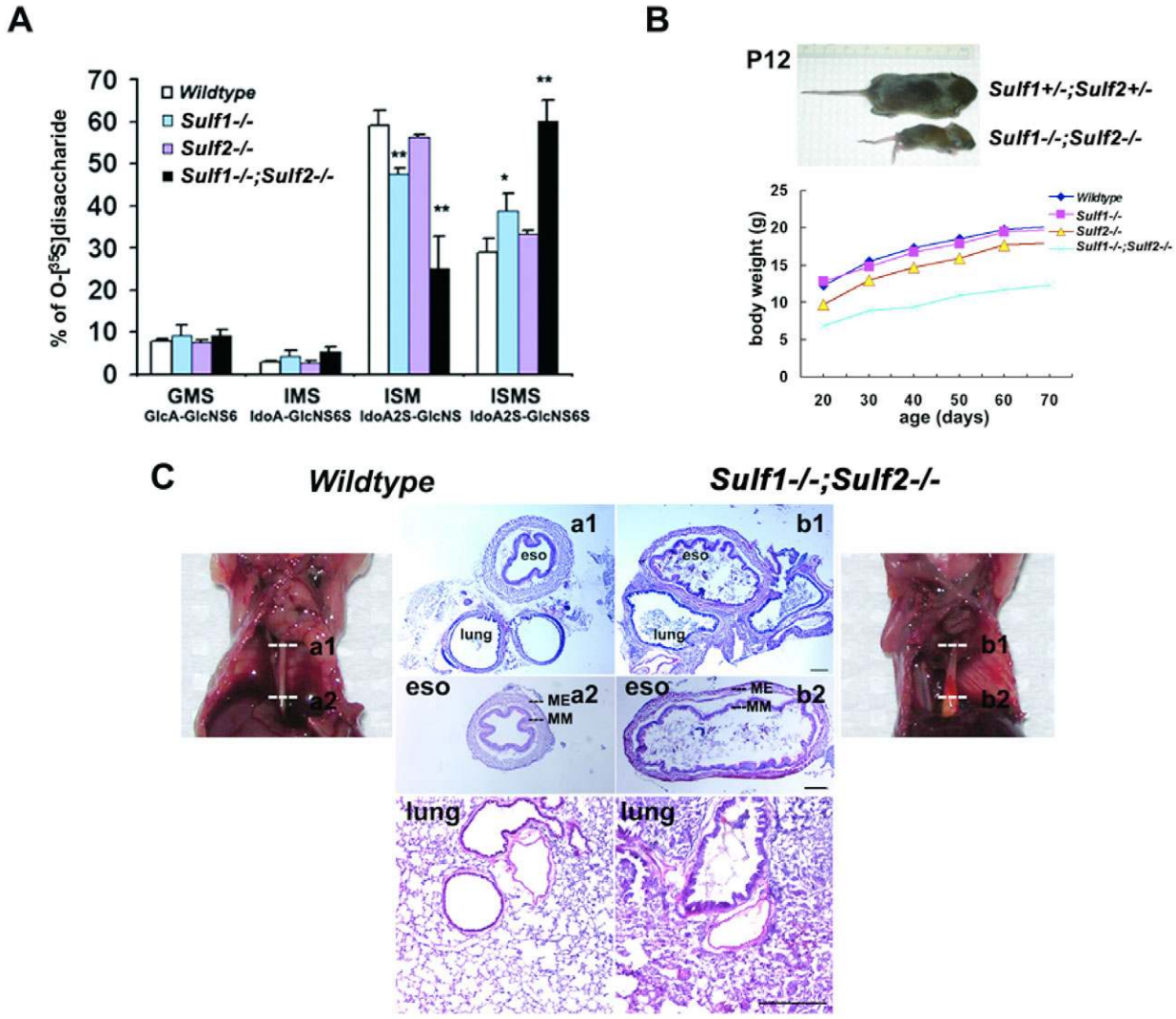

Fig. 1. *Sulf1*$^{-/-}$;*Sulf2*$^{-/-}$ mice have cellular HS 6-O-sulfation, postnatal growth and dysfunctional esophageal phenotypes. (**A**) Disaccharide analysis of HS. Radiolabeled HS was isolated from MEFs of wild-type, *Sulf1*$^{-/-}$, *Sulf2*$^{-/-}$ and *Sulf1*$^{-/-}$;*Sulf2*$^{-/-}$ embryos at E14.5, followed by disaccharide analysis. Individual disaccharides are represented as the percentage of the total radioactivity. Data presented are mean and standard deviation of a minimum of two independent samples of each genotype. In disaccharide abbreviation, M stands for the 2,5-anhydromannitol deamination products of GlcNS residues. **, $P<0.01$; *, $P<0.05$. (**B**) Comparison of the body size and weight between wild-type, *Sulf1*$^{-/-}$, *Sulf2*$^{-/-}$ and *Sulf1*$^{-/-}$;*Sulf2*$^{-/-}$ female mice at P12 and after weaning ($n=6$ for each group). (**C**) Histology of the adult esophagus and lung of wild-type control and *Sulf1*$^{-/-}$;*Sulf2*$^{-/-}$ mice. *Sulf1*$^{-/-}$;*Sulf2*$^{-/-}$ mice have enlarged esophagi with food accumulated inside (compare a1,a2 with b1,b2, respectively) and develop lung infections ($n=14$). Eso, esophagus; ME, muscularis externa; MM, muscularis mucosae. Scale bars: 100 μm.

Table 1. Summary of the general phenotypes of Sulf mutant mice

Genotype	% ISMS*	% Survival	Adult body weight	Fertility
Wild type	29±3.3	100	Normal	Normal
Sulf1$^{-/-}$	38±4.2†	100	Normal	Normal
Sulf2$^{-/-}$	33±0.7	100	~90%	Normal
Sulf1$^{+/-}$;*Sulf2*$^{+/-}$	34±0.7	100	Normal	Normal
Sulf1$^{-/-}$;*Sulf2*$^{+/-}$	46±3.1†	100	ND	Normal
Sulf1$^{+/-}$;*Sulf2*$^{-/-}$	59†	~90	70-90%	Reduced‡
Sulf1$^{-/-}$;*Sulf2*$^{-/-}$	61±5.1†	100 at birth, 45 at P21	40-70%	Much reduced§

ND, Not determined.
*The percentage of total O-^{35}S-labeled disaccharides generated after deaminative cleavage (pH 1.5) of purified HS. The M in ISMS (IdoA2S-GlcNS6S) stands for the 2,5-anhydromannitol deamination products of GlcNS residues.
$^{\dagger}P<0.01$.
‡Reduced in both sexes: the average litter size was 4-6, compared with the normal 8-10.
§Much reduced in both sexes: the average litter size was 2-4.

transcripts and polypeptides recognizable by anti-Sulf antibodies (see Fig. S1E and Fig. S2D in the supplementary material; data not shown), removal of exon 2 eliminates the full-length Sulf transcripts (see Fig. S1E and Fig. S2D in the supplementary material) and disrupts Sulf protein function, as shown by the disaccharide analyses of ^{35}S-radiolabeled glycosaminoglycans (GAGs) (Fig. 1A). GAGs were isolated from cultured primary mouse embryonic fibroblasts (MEFs) of the E14.5 skin that express both SULF1 and SULF2 (see Fig. S1E and Fig. S2D in the supplementary material). Loss of *Sulf1* selectively increased the abundance of the trisulfated disaccharide IdoA2S-GlcNS6S (ISMS), the known substrate of Sulf enzymes, by ~30% (Ai et al., 2003), and proportionately decreased the disulfated IdoA2S-GlcNS (ISM) disaccharide, whereas it had no effect on the other two disaccharides, GMS and IMS (Fig. 1A, Table 1). By contrast, *Sulf2*$^{-/-}$ and *Sulf1*$^{+/-}$;*Sulf2*$^{+/-}$ MEFs had unchanged levels of ISMS disaccharide, suggesting redundant Sulf protein activity in MEF cells. The magnitude of the increase in ISMS in various Sulf mutant MEFs was generally proportional to the number of mutant Sulf alleles (Table 1). Most significantly, HS isolated from *Sulf1*$^{-/-}$;*Sulf2*$^{-/-}$ MEFs had double the ISMS content (63%), a level comparable to that of heparin, a highly sulfated HS derivative. Sulf mutant MEFs of all genotypes had normal HS chain length, anionic properties, N-sulfation and chondroitin sulfate contents (data not shown). These results establish that Sulf mutants have loss-of-function mutations, and that Sulf enzymes are the major regulators of HS 6-O-sulfation in vivo.

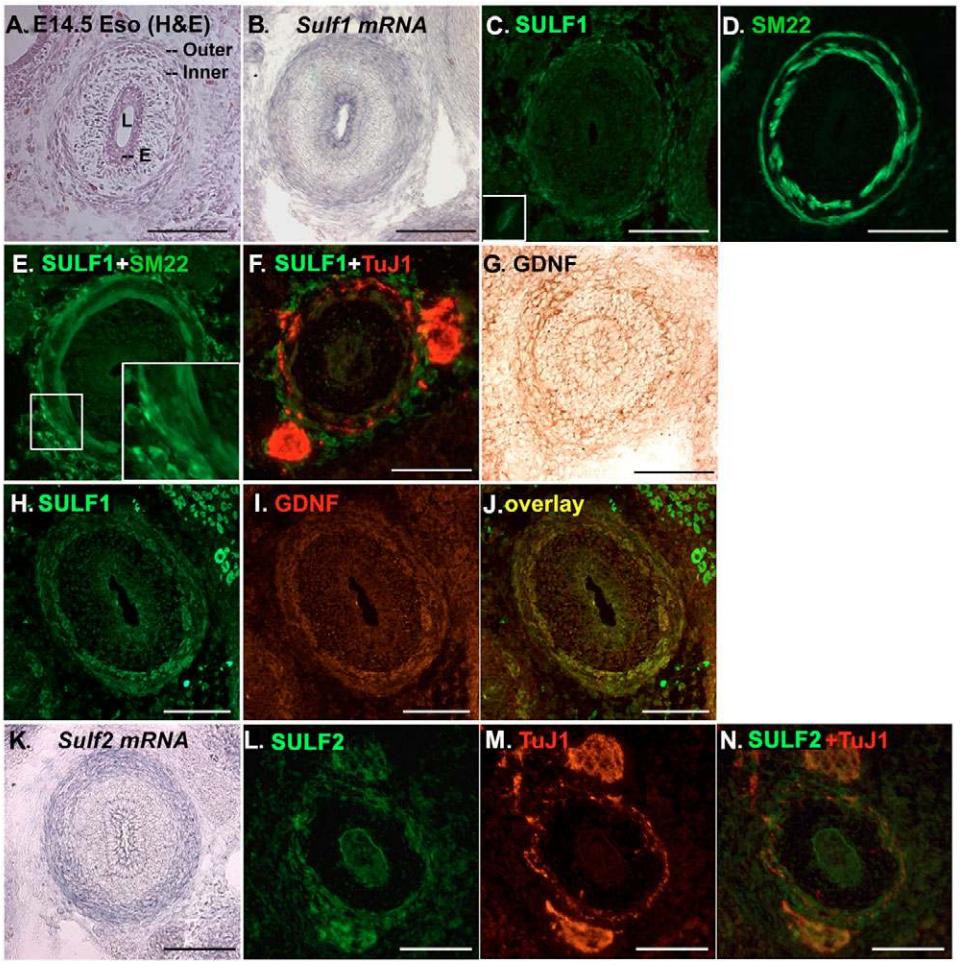

Fig. 2. SULF1 and SULF2 are differentially expressed in the embryonic esophagus. (**A-G**) SULF1 esophageal expression at E14.5. *Sulf1* mRNA (B) and protein (C) were detected at the outer layer of the esophagus and the protein was mostly on the cell surface (insert in C). The outer layer of the esophagus expresses SM22, a smooth muscle marker (D). Immunostaining with the rabbit anti-MS1HD antibody and the rabbit anti-SM22 antibody together identified SULF1 on the membrane of SM22-expressing cells (E); the insert shows a magnified image of the outlined staining. SULF1 did not colocalize with the TuJ1 staining (F). GDNF was detected diffusively across the esophageal muscle layers and partially overlapped with SULF1 in the outer layer (G). (**H-J**) SULF1 expression and colocalization with GDNF in the esophageal muscle layers at E16.5 by double staining. (**K-N**) SULF2 esophageal expression at E14.5. Cross-sections were double stained with SULF2 and TuJ1 antibodies. SULF2 tightly associated with TuJ1 staining. Scale bars: 100 μm.

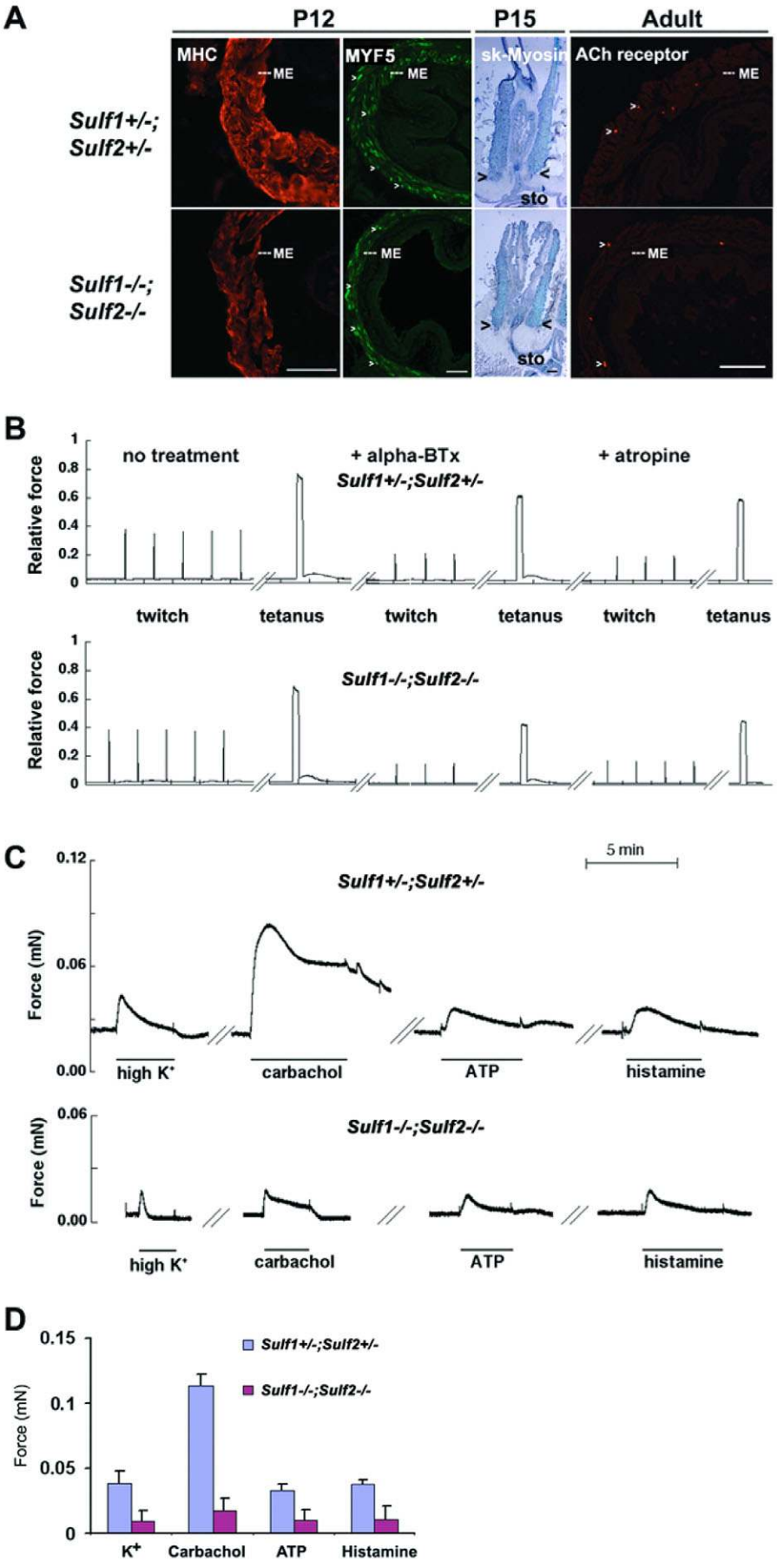

Fig. 3. The esophagi of *Sulf1*$^{-/-}$;*Sulf2*$^{-/-}$ mice have normal skeletal muscle function, but impaired smooth muscle contractility. (**A**) Postnatal development of the esophageal skeletal muscles in control and *Sulf1*$^{-/-}$;*Sulf2*$^{-/-}$ pups. The cross-sections of *Sulf1*$^{+/-}$;*Sulf2*$^{+/-}$ control and *Sulf1*$^{-/-}$;*Sulf2*$^{-/-}$ mice were immunostained with antibodies against skeletal muscle markers including myosin heavy chain (MHC) and MYF5 or incubated with Cy3-conjugated alpha-bungarotoxin (alpha-BTx) to identify acetylcholine (ACh) receptors on muscle. The completion of the esophageal skeletal muscle formation at P15 was assayed by immunostaining of the abdominal segments with an alkaline phosphatase-conjugated mouse antibody against fast skeletal myosin (sk-Myosin). The antigen-antibody complex was visualized using the substrate BM purple. Arrowheads mark the junction between the esophagus and the stomach. The *Sulf1*$^{-/-}$;*Sulf2*$^{-/-}$ esophagi have completed skeletal muscle formation in the esophagus at P15. Scale bars: 100 μm. (**B**) Physiological measurements of the esophageal skeletal muscles. The lower-half thoracic segments of the esophagi of the adult *Sulf1*$^{+/-}$;*Sulf2*$^{+/-}$ control and *Sulf1*$^{-/-}$;*Sulf2*$^{-/-}$ mice were subject to twitch and tetanus stimuli. Muscle contractility was measured and compared with those in the presence of selective ion-channel blockers (n=3). The *Sulf1*$^{-/-}$;*Sulf2*$^{-/-}$ esophagi exhibited comparable skeletal muscle contractility in response to the electrical stimuli and ion-channel blocks as the control esophagi. (**C**) Physiological tests of esophageal smooth muscle contractility. The smooth muscle of the control and the *Sulf1*$^{-/-}$;*Sulf2*$^{-/-}$ mutant esophagi were dissected and their contractile forces in response to various stimuli measured (n=3). The *Sulf1*$^{-/-}$;*Sulf2*$^{-/-}$ esophagi showed diminished smooth muscle contractility in response to carbachol, and partially reduced contractility in response to other chemicals. (**D**) Quantification of the esophageal smooth muscle contractility induced by various stimuli as shown in C.

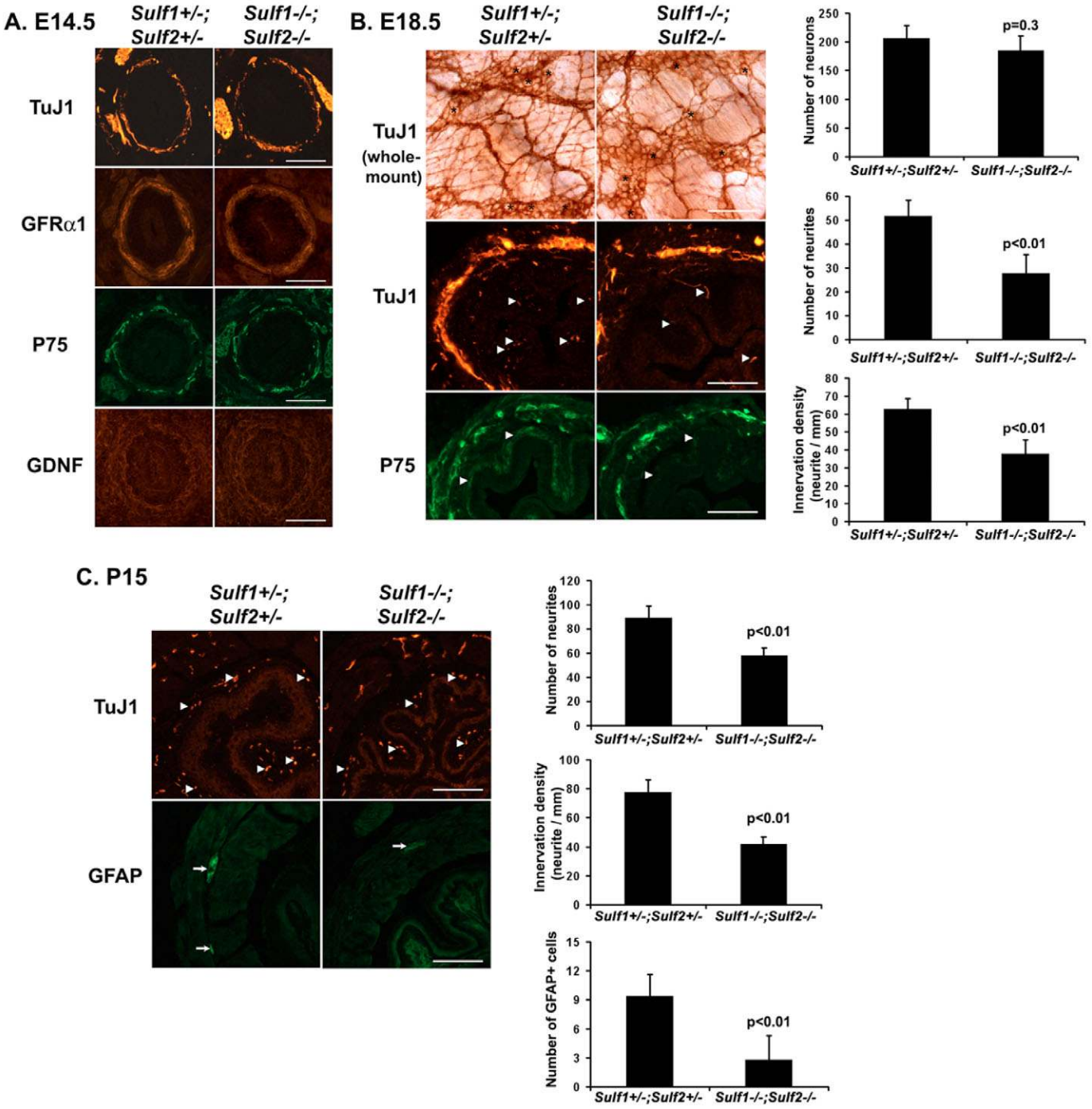

Fig. 4. See next page for legend.

The Sulf single-mutant mice are viable, fertile and have a normal life span of over 2 years (Fig. 1B, Table 1); however, *Sulf2*$^{-/-}$ mice weighed ~10% less than wild-type littermates. The *Sulf1*$^{-/-}$;*Sulf2*$^{-/-}$ embryos and neonates appeared normal at birth (data not shown) and fully viable based on observed mendelian frequencies at E11.5 (14/107, expected 1/8), at E14.5 (14/69, expected 1/4) and at birth (34/311, expected 1/8). We identified a primary developmental defect in esophageal innervation of *Sulf*$^{-/-}$;*Sulf2*$^{-/-}$ embryos that is likely to cause the severe postnatal growth defect of a majority of *Sulf1*$^{-/-}$;*Sulf2*$^{-/-}$ pups (41/76) that was evident as early as postnatal day 3 (P3) (Fig. 1B), with death at ~P14. *Sulf1*$^{-/-}$;*Sulf2*$^{-/-}$ pups that survived into adulthood (35/76) were runted and had greatly reduced fertility (Fig. 1B, Table 1). Approximately 60% of adult *Sulf1*$^{-/-}$;*Sulf2*$^{-/-}$ mice developed megaesophagus phenotypes as early as 2 months of age, characterized by food accumulation in the esophagus, coughing, labored breathing and lung infection (Fig. 1C). The esophagus of *Sulf1*$^{-/-}$;*Sulf2*$^{-/-}$ mice had an enlarged lumen with a normal arrangement of the muscle layers and esophageal epithelium by H&E staining and by immunostaining with specific markers for each cell type, although these tissue layers appeared much thinner owing to the dilation of the esophagus (Fig. 1C; data not shown). We did not observe inflammatory cells in the *Sulf1*$^{-/-}$;*Sulf2*$^{-/-}$ esophagi at P12 or in surviving adults (data not shown), ruling out

Fig. 4. The esophagi of *Sulf1*$^{-/-}$;*Sulf2*$^{-/-}$ mice have diminished neuronal innervation and enteric glial cells. The lower-half thoracic segments of the esophagus were immunolabeled either on cross-sections or by whole-mounts with various antibodies to examine neural innervation. (**A**) Comparable TuJ1 staining and expression of GFRα1, p75 and GDNF in *Sulf1*$^{+/-}$;*Sulf2*$^{+/-}$ control esophagi and *Sulf1*$^{-/-}$;*Sulf2*$^{-/-}$ esophagi at E14.5 (*n*=3). (**B**) Reduced neural innervation at the esophageal smooth muscle layer in *Sulf1*$^{-/-}$;*Sulf2*$^{-/-}$ esophagi at E18.5 (*n*=4). The whole esophagus was mounted on the glass slide after whole-mount immunohistochemistry with the TuJ1 antibody. One side of the flattened esophagus was photographed. The number of neurons (cell body marked by *) on one side of a 1-mm longitudinal segment was counted and four non-overlapping segments were counted for each esophagus. Numbers presented are the averages of the neural number per 1-mm segment. The innervation density at the smooth muscle layer was calculated by dividing the total number of innervating TuJ1$^+$ neurites (white arrowheads) on cross-sections by the circumference of smooth muscle. The circumference of the smooth muscle was not different between control and *Sulf1*$^{-/-}$;*Sulf2*$^{-/-}$ esophagi at E18.5 (control, 0.81±0.09 mm; mutant, 0.83±0.07 mm). A minimum of five serial cross-sections (200 μm apart) of each esophagus were quantified. The smooth muscle innervation was also shown by p75 staining (white arrowheads). *Sulf1*$^{-/-}$;*Sulf2*$^{-/-}$ esophagi had the same number of neurons as the control, whereas the smooth muscle innervation was reduced in *Sulf1*$^{-/-}$;*Sulf2*$^{-/-}$ esophagi. (**C**) Reduced esophageal innervation and enteric glial cells in *Sulf1*$^{-/-}$;*Sulf2*$^{-/-}$ esophagi at P15. Arrowheads indicate the TuJ1$^+$ neurites innervating the smooth muscle of muscularis mucosae. Arrows point to the enteric glial cells located between the skeletal muscle layers. The circumference of smooth muscle on cross-sections of *Sulf1*$^{-/-}$;*Sulf2*$^{-/-}$ esophagi (1.37±0.18 mm) was ~20% longer than that of littermate controls (1.15±0.13 mm). A minimum of 28 sections from four independent controls or *Sulf1*$^{-/-}$;*Sulf2*$^{-/-}$ mice were counted. Data shown in the bar graphs represent the number of TuJ1$^+$ neurites innervating smooth muscle, innervation density and the average number of enteric glial cells per cross-section. Statistics were calculated by two-tailed Student's *t*-test. Scale bars: 100 μm.

the possibility of immune cell-mediated tissue injury. In addition, we did not detect compensatory expression of the intact Sulf gene in single-mutant esophagi (data not shown).

SULF1 and SULF2 are differentially expressed in multiple embryonic tissues, including the esophagus

As the megaesophagus phenotype was prevalent only in *Sulf1*$^{-/-}$;*Sulf2*$^{-/-}$ mice, and not in *Sulf1*$^{-/-}$ (0%) or *Sulf2*$^{-/-}$ mice (~1-2%), this suggested that SULF1 and SULF2 have redundant functions that contribute to the megaesophagus phenotype in *Sulf1*$^{-/-}$;*Sulf2*$^{-/-}$ mice. To investigate this possibility, *Sulf1* and *Sulf2* expression in embryos was assayed by in situ hybridization and by immunostaining using specific antibodies generated against the hydrophilic domains of SULF1 (MS1HD) and SULF2 (MS2HD) (see Fig. S3A,B in the supplementary material). The tissue distribution of Sulf mRNA completely overlaps with protein expression, establishing the specificity of the Sulf antibodies (Fig. 1 and see Fig. S3C in the supplementary material) and consistent with Sulfs being membrane-docking and lacking free secretion (Dhoot et al., 2001). The expression levels of Sulfs were relatively low before E9.5 (data not shown). At E14.5 and E16.5, SULF1 and SULF2 were expressed at higher levels in partially overlapping patterns in a variety of embryonic tissues, including the floor plate of the neural tube, bone, cartilage, skeletal muscle and lung (see Fig. S3C in the supplementary material) (Lum et al., 2007).

SULF1 and SULF2 were found to be dynamically and differentially expressed in the embryonic esophagus (Fig. 2). They were first detectable around E11.5, peaked around E14.5, decreased dramatically by E18.5 and were undetectable 2 weeks after birth and in the adult (Fig. 2; data not shown). SULF1 expression did not co-localize with neuronal β-tubulin (TUBB3 – Mouse Genome Informatics), as labeled by the TuJ1 antibody (Fig. 2F). Instead, *Sulf1* mRNA and protein were detected at the esophageal ME at E14.5, when the smooth muscle forms prior to maturation into the skeletal muscle (Fig. 2B-E). To confirm muscle expression of SULF1, double labeling was performed with antibodies against SULF1 and the smooth muscle marker SM22 (TAGLN – Mouse Genome Informatics). Although both antibodies were raised in rabbit, we distinguished membrane-bound SULF1 from intracellular SM22 by their differential subcellular localization (Fig. 2C-E). We found that SULF1 outlined the membrane of SM22-expressing cells at the outer layer of E14.5 esophagus, and was localized at both outer and inner muscle layers of the esophagus at E16.5 (Fig. 2H and see Fig. S3D in the supplementary material). Esophageal muscle progenitors also express GDNF (Golden et al., 1999). To test whether SULF1 and GDNF co-localize, we characterized GDNF expression in the esophagus at E14.5 and E16.5 for comparison with SULF1 expression. GDNF was found on the cell surface and appeared diffusely across the esophageal ME at E14.5 (Fig. 2G), including the SULF1-expressing outer layer, and overlapped with SULF1 at E16.5 (Fig. 2H-J). By contrast, SULF2 was detected within the esophageal muscle layers and was tightly associated with the neuronal marker TuJ1 (Fig. 2K-N and see Fig. S3E in the supplementary material). As SULF2 and neuronal β-tubulin have differential subcellular localization, the observed close association between these two proteins indicates that SULF2 is expressed by innervating neuronal progenitors. The differential expression of SULF1 and SULF2 by muscle progenitors and by innervating neural progenitors suggests Sulf regulation of neuron-muscle interaction in the embryonic esophagi.

Esophagi of *Sulf1*$^{-/-}$;*Sulf2*$^{-/-}$ mice have impaired smooth muscle contractility

The esophageal defects in *Sulf1*$^{-/-}$;*Sulf2*$^{-/-}$ mice may result from impaired muscle contractility owing to defects in muscle maturation or in neuronal innervation. To distinguish these possibilities, we characterized the formation of the esophageal muscle (Fig. 2). The striated muscles of ME expressed the myogenic genes – including those encoding myosin heavy chain [MHC (MYHS)], MYF5, MYOD (MYOD1 – Mouse Genome Informatics) and myogenin – normally at P14, when *Sulf1*$^{-/-}$;*Sulf2*$^{-/-}$ pups start to die (Fig. 3A; data not shown). Also, *Sulf1*$^{-/-}$;*Sulf2*$^{-/-}$ esophagi complete skeletal muscle maturation normally at P15 (Rishniw et al., 2003), as shown by the expression of fast skeletal myosin in the esophageal abdominal segment connecting to the stomach (Fig. 3A). In addition, *Sulf1*$^{-/-}$;*Sulf2*$^{-/-}$ mice that survived into adulthood expressed fast skeletal muscle myosin and nicotinic acetylcholine receptor clusters normally in the esophageal striated muscle (Fig. 3A; data not shown). Furthermore, isolated thoracic longitudinal segments of the adult *Sulf1*$^{-/-}$;*Sulf2*$^{-/-}$ esophagi produced a comparable contractile force in response to twitch and tetanus electrical stimuli with those of controls (Fig. 3B) (Worl et al., 2002). To distinguish forces generated by nerve stimulation from forces generated from direct muscle stimulation, we applied alpha-bungarotoxin (alpha-Btx) to block electrical stimuli-

induced nerve input by inhibiting postsynaptic nicotinic acetylcholine receptors. Alpha-Btx significantly inhibited both twitch and tetanus forces in both *Sulf1*$^{-/-}$;*Sulf2*$^{-/-}$ and control esophagi in a similar manner, demonstrating that the skeletal muscle innervation is normal in *Sulf1*$^{-/-}$;*Sulf2*$^{-/-}$ esophagi. After the treatment with alpha-BTx, the remaining forces were resistant to atropine, an inhibitor of muscarinic receptors on smooth muscle (Fig. 3B), but were completely inhibited by further addition of tetrodotoxin in *Sulf1*$^{-/-}$;*Sulf2*$^{-/-}$ and control esophagi (data not shown). These results establish that the electrical stimuli-induced forces are produced largely by skeletal muscle, not by smooth muscle, in the esophagus. The electrical stimuli elicited relatively low levels of smooth muscle contractility, as evidenced by the small shoulders after the tetanus stimuli and by their sensitivity to inhibition by atropine (Fig. 3B). We observed no significant difference in skeletal muscle contractility between the double-mutant and control esophagi. Therefore, the development, maturation and function of esophageal skeletal muscle is unaffected in *Sulf1*$^{-/-}$;*Sulf2*$^{-/-}$ mice.

By contrast, smooth muscle contractility was found to be impaired in *Sulf1*$^{-/-}$;*Sulf2*$^{-/-}$ esophagi. The contractile forces of the isolated smooth muscle ring at the thoracic segments of the esophagi were elicited by various stimuli such as electrical, high K^+, carbachol, ATP and histamine (Storr et al., 2001; Worl et al., 2002). The smooth muscle contractility elicited by electrical stimuli (the small shoulders after tetanus stimuli, Fig. 3B) was comparable in control and *Sulf1*$^{-/-}$;*Sulf2*$^{-/-}$ mutant esophagi. In addition, compared with *Sulf1*$^{+/-}$;*Sulf2*$^{+/-}$ controls, the *Sulf1*$^{-/-}$;*Sulf2*$^{-/-}$ esophageal smooth muscles showed a greatly diminished response to carbachol, an agonist of the muscarinic receptor, but only partially reduced response to other stimuli (Fig. 3C,D). A similar decrease in carbachol-induced smooth muscle contractility was observed in *Sulf1*$^{-/-}$;*Sulf2*$^{-/-}$ esophagi at P15 (data not shown). No smooth muscle contractility defects were observed in the lower sphincter muscle of the *Sulf1*$^{-/-}$;*Sulf2*$^{-/-}$ esophagi (data not shown). The esophageal defects of *Sulf1*$^{-/-}$;*Sulf2*$^{-/-}$ mice are different from symptoms of achalasia in which the lower sphincter muscle contractility is deregulated owing to a loss of inhibitory nitrinergic neurons (Longstretch and Walker, 1994; Holland et al., 2002; Neuhuber et al., 2006), but are similar to those observed in congenital idiopathic megaesophagus. Carbachol-induced smooth muscle contractility is likely to correlate with the level of neuronal innervation in the esophagus, as shown in studies of sprouty 2 mutant mice (Taketomi et al., 2005). The selective impairment in carbachol-induced smooth muscle contractility of the *Sulf1*$^{-/-}$;*Sulf2*$^{-/-}$ esophagi therefore suggests specific neuronal innervation defects rather than a general disruption of the smooth muscle structure in the muscularis mucosae.

Neuronal innervation and enteric glial cell numbers are reduced in the esophagi of *Sulf1*$^{-/-}$;*Sulf2*$^{-/-}$ mice

To test whether esophageal innervation is defective in *Sulf1*$^{-/-}$;*Sulf2*$^{-/-}$ mice, we identified innervating nerve fibers of both intrinsic and extrinsic neurons using the TuJ1 antibody. At E14.5, before the neurites extend across the ME, the *Sulf1*$^{+/-}$;*Sulf2*$^{+/-}$ control and *Sulf1*$^{-/-}$;*Sulf2*$^{-/-}$ esophagi exhibited comparable staining with TuJ1, GDNF, GDNF receptor α 1 (GFRα1), RET (previously known as c-RET), or the low-affinity neurotrophin receptor p75 (NGFR – Mouse Genome Informatics) (Fig. 4A; data not shown). However, at E18.5, *Sulf1*$^{-/-}$;*Sulf2*$^{-/-}$ esophagi had much reduced levels of neurite sprouting and innervation density at the smooth muscle of the muscularis mucosae, although the number of intrinsic neurons and the circumference of the esophagi were unchanged (Fig. 4B). In addition, we found no difference in p75 expression on the cell body or in the number of p75-expressing intrinsic neurons between control and *Sulf1*$^{-/-}$;*Sulf2*$^{-/-}$ esophagi (Fig. 4B). However, p75 expression on neurites innervating the smooth muscle was decreased in *Sulf1*$^{-/-}$;*Sulf2*$^{-/-}$ esophagi, providing additional evidence that the innervation of the muscularis mucosae is defective. Reduced smooth muscle innervation in *Sulf1*$^{-/-}$;*Sulf2*$^{-/-}$ esophagi persisted postnatally and in the adult (Fig. 4C and see Fig. S4 in the supplementary material), which directly affected smooth muscle contractility (Fig. 3C,D) and led to gradual enlargement of the esophageal lumen from a ~20% increase in the circumference of smooth muscle at P15 (Fig. 4C), to almost a doubling in the circumference in adults (Fig. 1C and see Fig. S4 in the supplementary material).

To test whether enteric glial cells might also be affected in mutant esophagi, we labeled the esophagus using antibodies against the glial cell markers, glial fibrillary acidic protein (GFAP) and S100 (S100a1 – Mouse Genome Informatics) at P15 and in the adult when enteric glial cells form and mature (Fig. 4C and see Fig. S4 in the supplementary material; data not shown). We found that the number of GFAP-expressing cells along the thoracic segments of the *Sulf1*$^{-/-}$;*Sulf2*$^{-/-}$ esophagi was reduced to one-third and to half of that in the control esophagi at P15 and in adult, respectively (Fig. 4C and see Fig. S4 in the supplementary material). Since esophageal innervation is controlled by GDNF (Yan et al., 2004) and GDNF supports enteric glial differentiation from neural crest progenitors (Heuckeroth et al., 1998), the observed esophageal defects in *Sulf1*$^{-/-}$;*Sulf2*$^{-/-}$ mice suggest that Sulf regulation of the GDNF signaling pathway establishes the esophageal innervation that is required for postnatal feeding and growth.

SULF1 and SULF2 are required for GDNF-dependent neurite outgrowth in embryonic esophageal explants

To investigate whether SULF1 and SULF2 are required for GDNF-induced neurite outgrowth of the endogenous neurons in the embryonic esophagus, esophageal explants from E11.5 embryos were cultured on collagen gels (Yan et al., 2004). After 4 days, the explants adhered to the collagen gel and exhibited a GDNF dose-dependent neurite sprouting, as shown by TuJ1 immunoreactivity extending from the explants in GDNF-induced cultures (Fig. 5A). The sprouting was not promoted by neurotrophins NGF (NGFβ – Mouse Genome Informatics), BDNF, NT3 (NTF3), NT4 (NTF5) or any other previously known Sulf-regulated signaling ligand, including FGF2, HGF, VEGF165 (NRP1), Wnts, BMP2 and sonic hedgehog (Fig. 5A-C and see Fig. S6 in the supplementary material) (Ai et al., 2005). Furthermore, heparin, but not dermatan sulfate, blocked the GDNF-induced neurite outgrowth (see Fig. S6A,B in the supplementary material), establishing the HS-dependent GDNF activity. The neurite outgrowth from control esophageal explants could be induced by GDNF at 10 ng/ml, with maximal induction at 50 ng/ml GDNF (Fig. 5A,C). By contrast, *Sulf1*$^{-/-}$;*Sulf2*$^{-/-}$ explants failed to extend neurites at 10 ng/ml GDNF, and the neurite outgrowth was less than half of the control levels at 20 ng/ml. The defect in the neurite outgrowth of *Sulf1*$^{-/-}$;*Sulf2*$^{-/-}$ esophageal explants was fully rescued by 100 ng/ml GDNF (Fig. 5A,C). A lack of neurite outgrowth by *Sulf1*$^{-/-}$;*Sulf2*$^{-/-}$ esophageal explants at 10 ng/ml GDNF could be due to disrupted GDNF signaling in intrinsic neurons, or to a reduction in the number of intrinsic neurons. To distinguish between these two possibilities, we quantified the total number of TuJ1-immunoreactive intrinsic neurons within the

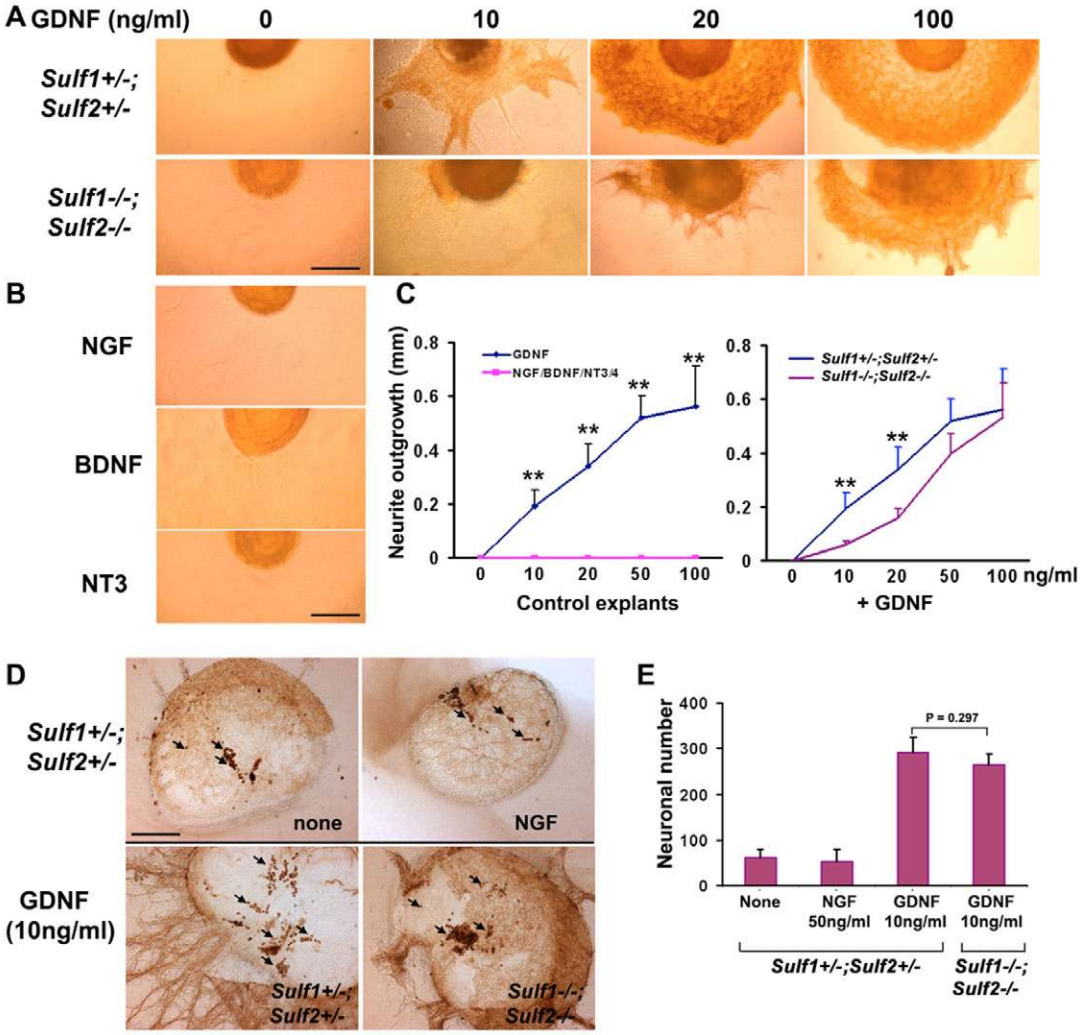

Fig. 5. *Sulf1*$^{-/-}$;*Sulf2*$^{-/-}$ esophagi have defective GDNF-dependent neurite outgrowth. Esophagi (~400 μm) were dissected from E11.5 embryos and plated on collagen gel containing BSA, GDNF or neurotrophins at various concentrations. After 4 days, the whole explant was immunostained with the TuJ1 antibody. Explants that failed to attach to collagen gel were not included in the assay. (**A**,**B**) Neurite outgrowth of E11.5 esophageal explants was selectively dependent on GDNF, but not on neurotrophin. *Sulf1*$^{-/-}$;*Sulf2*$^{-/-}$ esophagi failed to extend neurites at 10 ng/ml GDNF and showed reduced neurite outgrowth at 20 ng/ml and 50 ng/ml GDNF. (**C**) Quantification of the neurite outgrowth shown in A and B. The length of the extended neurite was measured along six axes, 30° apart and the average was calculated to represent the neurite outgrowth of one explant. Data represent the mean and the standard deviation of a minimum of four individual cultures. (**D**,**E**) Quantification of the total number of neurons in the explants. The neurons in the explants (dark cell-body staining by the TuJ1 antibody, indicated by arrows) were quantified using the bright field at low magnitude. Neurons were scattered, or even migrated out of the control explants in the presence of 10 ng/ml GDNF. In control explants cultured in the presence of BSA or NGF and in GDNF-treated *Sulf1*$^{-/-}$;*Sulf2*$^{-/-}$ explants, neurons tended to form clusters. The large clusters of neurons in *Sulf1*$^{-/-}$;*Sulf2*$^{-/-}$ explants were quantified by summing the neuronal numbers at different focal planes. **, $P<0.01$ (two-tailed Student's *t*-test). Scale bars: 250 μm in A,B; 100 μm in D.

explants after 4 days in culture. We found that GDNF is essential for neuron number, as control explants cultured without any neurotrophic factors or in the presence of NGF had only one-third of the neurons as explants treated with 10 ng/ml GDNF (Fig. 5E). *Sulf1*$^{-/-}$;*Sulf2*$^{-/-}$ esophageal explants, although they showed no significant neurite outgrowth at 10 ng/ml GDNF, had the same number of intrinsic neurons as the controls (Fig. 5E), consistent with the in vivo phenotype. In addition, a few neurons within GDNF-treated control explants migrated out of the explants (data not shown), whereas neurons of the *Sulf1*$^{-/-}$;*Sulf2*$^{-/-}$ explants never migrated out of the explants (Fig. 5D), suggesting a defect in GDNF-induced neural migration.

SULF1 and SULF2 regulate GDNF signaling for esophageal function

To investigate mechanisms of Sulf regulation of GDNF signaling, we utilized biochemical and tissue culture assays. SULF1 and GDNF are co-expressed by the esophageal muscle progenitors and their expression levels are co-regulated to peak between E14 and E16 (Golden et al., 1999), suggesting that they have related functions. To test whether SULF1 regulates GDNF signaling, we first examined whether SULF1 modulates GDNF binding to HS by comparing GDNF binding to heparin-agarose beads that were predigested with either purified SULF1 or enzymatically inactive QSULF1(C-A) (Fig. 6A) (Ai et al., 2003). SULF1 activity significantly decreased GDNF

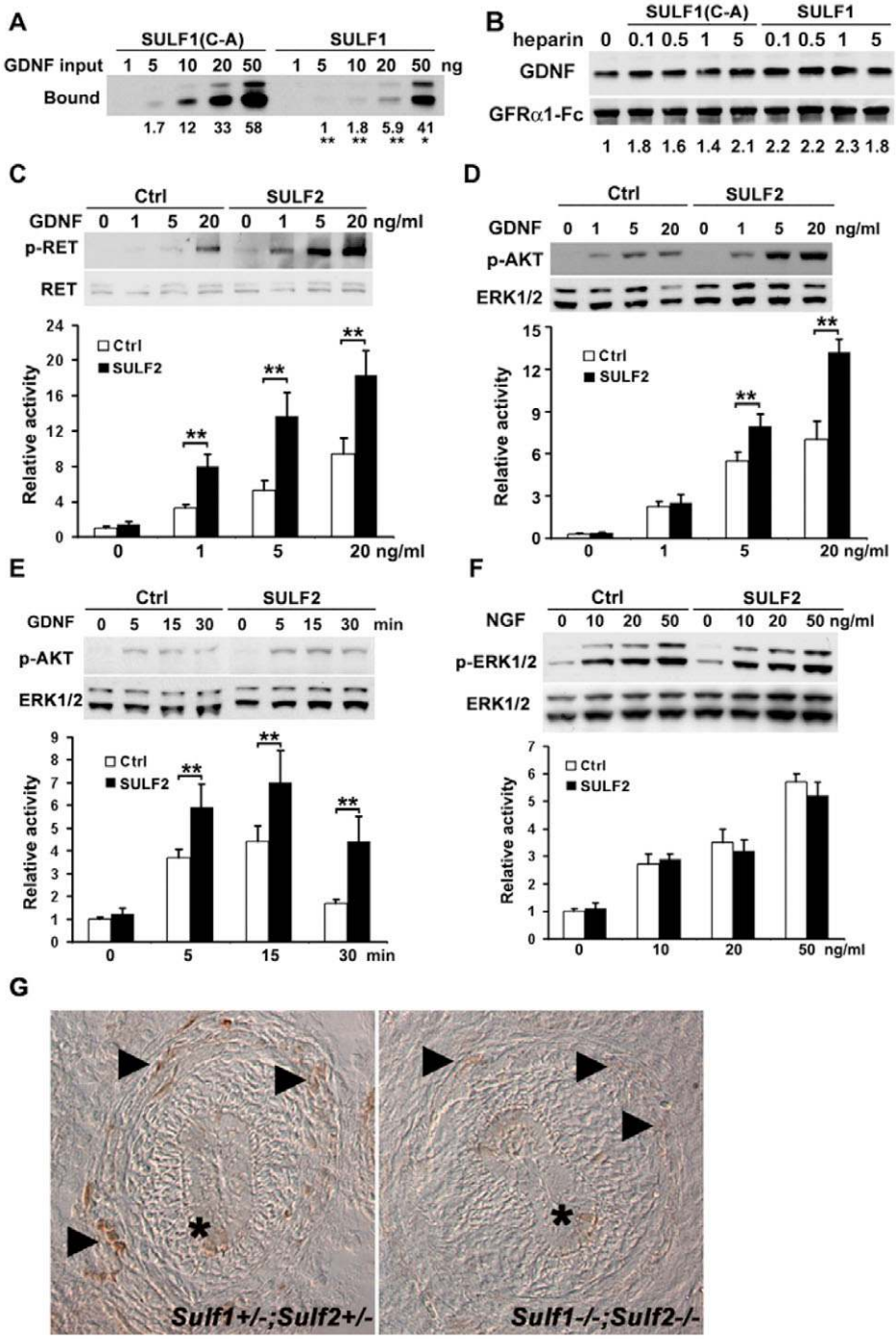

Fig. 6. SULF1 and SULF2 regulate GDNF binding to heparin and the GDNF signaling activity. (**A**) SULF1 reduces GDNF binding to heparin. Heparin conjugated to agarose beads was digested by SULF1 or inactive QSULF1(C-A) control. Various amounts of GDNF were incubated with enzyme-digested heparin beads (20 μl) to allow binding. The amount of GDNF bound to the beads was assayed by western blot. The intensity of individual bands was quantified by Multi-analysis software (Bio-Rad). Numbers listed beneath each lane are normalized quantification of the individual bands from three independent experiments. (**B**) SULF1 has no effect on GDNF binding to GFRα1. Heparin predigested either by SULF1 or inactive QSULF1(C-A) was added to a mixture of GDNF (10 ng) and GFRα1-Fc (1 μg) to allow GDNF-heparin-GFRα1-Fc ternary complex formation. The complex was pulled down by protein A-agarose beads. The amount of GDNF bound to GFRα1 was assayed by western blot and normalized to the amount of GFRα1. (**C-E**) SULF2 enhances the GDNF signaling activity. NG108-15 cells that were stably transfected with the control vector or the SULF2 expression vector were stimulated by GDNF for 5 minutes, or by GDNF (5 ng/ml) for various lengths of time. The activation of GDNF signaling pathway was analyzed by assaying the phosphorylation of RET (at tyrosine, p-RET) and of the downstream AKT (p-AKT) by western blot. Total RET or Erks were used as loading control. Data shown are controlled for loading and then normalized to the basal level of control cells. (**F**) SULF2 had no effect on NGF signaling in PC12 cells. Serum-starved PC12 cells that stably expressed SULF2 or inactive QSULF1(C-A) were treated with NGF. The activation of NGF signaling was analyzed by assaying the phosphorylation of downstream Erks (p-Erk). Data presented are the mean and standard deviation of a minimum of three independent experiments. **, $P<0.01$, * $P<0.05$ (two-tailed Student's *t*-test). (**G**) *Sulf* double-mutant esophagi have reduced MAPK phosphorylation in the intrinsic neurons. E14.5 esophageal sections were immunostained with an antibody against phosphorylated MAPK. Arrowheads point to phosphorylated MAPK immunoreactivity in neuronal cell bodies within the muscle layers. Asterisks mark the endothelial cells with phosphorylated MAPK immunoreactivity.

binding to heparin by up to 6-fold at sub-saturating amounts of GDNF, and by ~30% under conditions of excess GDNF (Fig. 6A). Second, we tested whether SULF1 activity affects HS-regulated GDNF binding to GFRα1. GDNF and the extracellular domain of GFRα1 (GFRα1-Fc) were incubated with various amounts of heparin predigested by SULF1 or enzymatically inactive QSULF1(C-A) to allow the formation of a GDNF-heparin-GFRα1-Fc ternary complex. As reported previously, heparin enhanced GDNF binding to GFRα1 by 2-fold (Fig. 6B) (Rickard et al., 2003). However, SULF1 had no effect in heparin-regulated GDNF binding to GFRα1 (Fig. 6B), indicating that SULF1-regulated HS 6-O-desulfation does not control GDNF binding to GFRα1. These findings suggest that SULF1 functions in the embryonic esophagus to control the affinity of GDNF for HS in the extracellular matrix to facilitate GDNF binding to RET receptor on GDNF-responding innervating neurons.

SULF2 is expressed by esophageal muscle-innervating neurons and thus may regulate the response of these neurons to GDNF. To test whether SULF2 regulates signaling activity of GDNF in

neurons, we established stably transfected neuroblastoma-glioma NG108-15 cell lines that expressed comparable levels of SULF2 or inactive QSULF1(C-A) (data not shown), or an empty expression vector. NG108-15 cells do not express detectable levels of endogenous Sulfs, as judged by immunostaining (data not shown). In response to GDNF, NG108-15 cells showed dose-dependent activation of the signaling pathway by phosphorylating the RET receptor and the downstream kinases AKT (also known as PKB and AKT1 – Mouse Genome Informatics) and Erks (MAPK1) 3- to 10-fold above uninduced levels (Fig. 6C,D and see Fig. S5 in the supplementary material). Expression of SULF2, but not inactive QSULF1(C-A) or empty vector, further increased the phosphorylation levels of RET and AKT by 2- to 3-fold and Erks by up to 2-fold in response to GDNF (Fig. 6C,D and see Fig. S5A in the supplementary material). Additionally, SULF2-expressing NG108-15 cells showed sustained activation of downstream AKT and Erks over 30 minutes after GDNF stimulation, compared with controls in which GDNF activity rapidly declined 15 minutes after stimulation (Fig. 6E and see Fig. S5B in the supplementary material). By contrast, SULF2 had no effect on NGF-induced phosphorylation of AKT or Erks in PC12 cells (Fig. 6F), demonstrating the functional specificity of SULF2 in the GDNF signaling pathway. This result is also consistent with previous findings that NGF signaling is independent of HS sulfation (Barnett et al., 2002). These studies of neural cell lines provide evidence that SULF2 enhances GDNF signaling in neural progenitors during esophageal innervation.

To further demonstrate that Sulfs enhance GDNF signaling in vivo, we assayed the endogenous level of MAPK activation in E14.5 esophagi by immunohistochemistry. Compared with robust MAPK phosphorylation in cell bodies located within the control esophageal muscles, *Sulf1*$^{-/-}$;*Sulf2*$^{-/-}$ enteric neurons showed a much reduced level of MAPK phosphorylation (Fig. 6G). By contrast, *Sulf1*$^{-/-}$;*Sulf2*$^{-/-}$ epithelial cells surrounding the esophageal lumen exhibited normal MAPK phosphorylation (Fig. 6G). Although MAPK phosphorylation can be triggered by several signals, the GDNF pathway is one of the major signaling pathways in esophageal neuronal progenitors at E14.5. Therefore, this observation is consistent with our finding that Sulfs promote GDNF signaling activity, as shown by esophageal explant and cell signaling assays.

DISCUSSION

In this study, we have utilized gene targeting in combination with physiological, biochemical and cell biological approaches to investigate functions of Sulfs and HS 6-O-sulfated sequences in developmental signaling. Our results reveal a novel regulatory function of Sulfs in GDNF signaling during esophageal innervation, and thus provide the first evidence that Sulfs are essential in vivo regulators of HS-mediated developmental signaling. Mechanistically, we show that Sulf activity decreases GDNF binding to HS, which promotes signaling. This result suggests that Sulfs have dual functions: to control the binding of GDNF to cell surface and matrix and to regulate neuronal reception of the GDNF signal at the receptor level. Sulf activity is not sufficient to release GDNF from the extracellular matrix, as E14.5 Sulf double-mutant esophagi have normal GDNF immunoreactivity (Fig. 4A). One attractive model is that SULF1 would mobilize GDNF in the matrix by reducing the non-specific GDNF-HS interaction, thereby promoting GDNF transmission from esophageal muscle to innervating neurons and facilitating high-affinity receptor interaction and signaling response in GDNF-receiving neurons.

Our studies also show that Sulfs are enhancers of GDNF signaling rather than obligatory components in the GDNF pathway. Neuroblastoma-glioma cells, which do not express Sulfs, are capable of transmitting the GDNF signal. In addition, high concentrations of GDNF rescue the neurite outgrowth defect of Sulf mutant esophagi in our explant assays, demonstrating that Sulf-deficient neurons are competent to receive GDNF signal. The regulatory roles of Sulfs in GDNF signaling contrast with the obligatory roles of GDNF or GDNF receptors, as demonstrated by the observed differences in the number of enteric neurons between Sulf mutant mice and mice deficient in GDNF or GDNF receptors (Baloh et al., 2000). In addition, we did not observe any significant innervation defects in the Sulf double-mutant colon by immunolabeling (see Fig. S7 in the supplementary material). These findings suggest that Sulf activity is not crucial for enteric neural crest progenitor migration or myenteric plexus formation during development, consistent with the relatively late onset of Sulf expression. However, Sulfs are essential for the developmental transmission of GDNF signaling during esophageal innervation in the embryo. The esophageal smooth muscle is largely innervated by intrinsic neurons. Although extrinsic innervation might also be affected, the observed ~50% reduction of smooth muscle innervation in Sulf double-mutant esophagi indicates Sulf function in intrinsic neurons, which is consistent with the defects in GDNF-dependent neurite outgrowth of the Sulf mutant esophageal explants.

As Sulf-deficiency leads to specific changes in HS 6-O-sulfation without disrupting the overall charge or structure of HS chains, our findings establish that Sulf desulfation generates HS with a distinct 6-O-sulfated fine structure – an 'HS code' – to control the specificity of extracellular signaling responses to HS-dependent ligands and receptors. HS 6-O-sulfation is known to be strictly controlled by developmental stage, tissue type and in tumors (Esko and Lindahl, 2001; Kreuger et al., 2006). Here, we show that Sulfs have dynamic expression and are enzymatically active in embryos, indicating their dynamic regulatory roles. Sulf mutant mice not only provide new tools for studies to decipher the HS-sulfation code for regulation of ligand-receptor interactions, but also open new opportunities to investigate the genetic and developmental signaling mechanisms underlying the motility disorder, congenital idiopathic megaesophagus. Additionally, Sulf mutant mice provide a new therapeutic model for developmental investigations of GDNF-mediated neuroprotection in Parkinson's disease and brain injury (Airaksinen and Saarma, 2002) and in other diseases involving Sulf-mediated HS-regulated signaling.

We thank Dr Mario Gimona for providing SM22 antibody, Drs Sarah Wilcox-Adelman, Jennifer Chen, Cathy Soula and Willington Cardoso for helpful discussion, Monika Kimanova for generating mouse chimeras and Aliete Langsdorf for maintaining mouse colonies. This work was supported by a grant from the National Institute of Child Health and Human Development to C.P.E., a National Institute of Health postdoctoral fellowship to X.A. and a grant (#13401) from the Swedish Research Council to M.K.-G. The authors declare that they have no conflicting financial interests.

Supplementary material

Supplementary material for this article is available at
http://dev.biologists.org/cgi/content/full/134/18/3327/DC1

References

Ai, X., Do, A., Lozynska, O., Kusche-Gullberg, M., Lindahl, U. and Emerson, C. P., Jr (2003). QSulf1 remodels the 6-O sulfation states of cell surface heparan sulfate proteoglycans to promote Wnt signaling. *J. Cell Biol.* **162**, 341-351.

Ai, X., Kusche-Gullberg, M., Lindahl, U. and Emerson, C. P., Jr (2005). Remodeling of heparan sulfate sulfation by extracellular endosulfatases. In *Chemistry and Biology of Heparin and Heparan Sulfate* (ed. H. G. Garg, R. J. Linhardt and C. A. Hales), pp. 245-258. New York: Elsevier.

Ai, X., Do, A., Kusche-Gullberg, M., Lindahl, U., Lu, K. and Emerson, C. P., Jr (2006). Substrate specificity and domain functions of extracellular heparan sulfate 6-O-endosulfatases, QSulf1 and QSulf2. *J. Biol. Chem.* **281**, 4969-4976.

Airaksinen, M. S. and Saarma, M. (2002). The GDNF family: signaling, biological functions and therapeutic value. *Nat. Rev. Neurosci.* **3**, 383-394.

Baloh, R. H., Enomoto, H., Johnson, E. M., Jr and Milbrandt, J. (2000). The GDNF family ligands and receptors – implications for neural development. *Curr. Opin. Neurobiol.* **10**, 103-110.

Barnett, M. W., Fisher, C. E., Perona-Wright, G. and Davies, J. A. (2002). Signalling by glial cell line-derived neurotrophic factor (GDNF) requires heparan sulphate glycosaminoglycan. *J. Cell Sci.* **115**, 4495-4503.

Breuer, C., Neuhuber, W. L. and Worl, J. (2004). Development of neuromuscular junctions in the mouse esophagus: morphology suggests a role for enteric coinnervation during maturation of vagal myoneural contacts. *J. Comp. Neurol.* **475**, 47-69.

Danesin, C., Agius, E., Escalas, N., Ai, X., Emerson, C. P. and Soula, C. (2006). Ventral neural progenitors switch toward an oligodendroglial fate in response to increased sonic hedgehog (Shh) activity: involvement of sulfatase 1 in modulating Shh signaling in the ventral spinal cord. *J. Neurosci.* **26**, 5037-5048.

Dhoot, G. K., Gustafsson, M. K., Ai, X., Sun, W., Standiford, D. M. and Emerson, C. P., Jr (2001). Regulation of Wnt signaling and embryo patterning by an extracellular sulfatase. *Science* **293**, 1663-1666.

Durbec, P. L., Larsson-Blomberg, L. B., Schuchardt, A., Costantini, F. and Pachnis, V. (1996). Common origin and developmental dependence on c-ret of subsets of enteric and sympathetic neuroblasts. *Development* **122**, 349-358.

Esko, J. D. and Lindahl, U. (2001). Molecular diversity of heparan sulfate. *J. Clin. Invest.* **108**, 169-173.

Golden, J. P., DeMaro, J. A., Osborne, P. A., Milbrandt, J. and Johnson, E. M., Jr (1999). Expression of Neurturin, GDNF, and GDNF family-receptor mRNA in the developing and mature mouse. *Exp. Neurol.* **158**, 504-528.

Heuckeroth, R. O., Lampe, P. A., Johnson, E. M. and Milbrandt, J. (1998). Neurturin and GDNF promote proliferation and survival of enteric neuron and glial progenitors in vitro. *Dev. Biol.* **200**, 116-129.

Holland, C. T., Satchell, P. M. and Farrow, B. R. (2002). Selective vagal afferent dysfunction in dogs with cogenital idiopathic megaesophagus. *Auton. Neurosci.* **99**, 18-23.

Kamikawa, Y. and Shimo, Y. (1979). Cholinergic and adrenergic innervations of the muscularis mucosae in guinea-pig esophagus. *Arch. Int. Pharmacodyn. Ther.* **238**, 220-232.

Kreuger, J., Spillmann, D., Li, J. P. and Lindahl, U. (2006). Interactions between heparan sulfate and proteins: the concept of specificity. *J. Cell Biol.* **174**, 323-327.

Lamanna, W. C., Baldwin, R. J., Padva, M., Kalus, I., Ten Dam, G., van Kuppevelt, T. H., Gallagher, J. T., von Figura, K., Dierks, T. and Merry, C. L. (2006). Heparan sulfate 6-O-endosulfatases: discrete in vivo activities and functional co-operativity. *Biochem. J.* **400**, 63-73.

Lin, X. (2004). Functions of heparan sulfate proteoglycans in cell signaling during development. *Development* **131**, 6009-6021.

Longstretch, G. F. and Walker, F. D. (1994). Megaesophagus and hereditary nervous system degeneration. *J. Clin. Gastroenterol.* **19**, 125-127.

Lum, D. H., Tan, J., Rosen, S. D. and Werb, Z. (2007). Gene trap disruption of the mouse heparan sulfate 6-O-endosulfatase gene, Sulf2. *Mol. Cell. Biol.* **27**, 678-688.

Morimoto-Tomita, M., Uchimura, K., Werb, Z., Hemmerich, S. and Rosen, S. D. (2002). Cloning and characterization of two extracellular heparin-degrading endosulfatases in mouse and human. *J. Biol. Chem.* **277**, 49175-49185.

Neuhuber, W. L., Raab, M., Worl, J. and Berthoud, H. R. (2006). Innervation of the mammalian esophagus. *Adv. Anat. Embryol. Cell Biol.* **185**, 1-73.

Rickard, S. M., Mummery, R. S., Mulloy, B. and Rider, C. C. (2003). The binding of human glial cell line-derived neurotrophic factor to heparin and heparan sulfate: importance of 2-O-sulfate groups and effect on its interaction with its receptor, GFRα1. *Glycobiology* **13**, 419-426.

Rishniw, M., Xin, H., Deng, K. and Kotlikoff, M. I. (2003). Skeletal myogenesis in the mouse esophagus does not occur through transdifferentiation. *Genesis* **36**, 81-82.

Sang, Q. and Young, H. M. (1997). Development of nicotinic receptor clusters and innervation accompanying the change in muscle phenotype in the mouse esophagus. *J. Comp. Neurol.* **386**, 119-136.

Sang, Q. and Young, H. M. (1998). The origin and development of the vagal and spinal innervation of the external muscle of the mouse esophagus. *Brain Res.* **809**, 253-268.

Storr, M., Geisler, F., Neuhuber, W. L., Schusdziarra, V. and Allescher, H. D. (2001). Characterization of vagal input to the rat esophageal muscle. *Auton. Neurosci.* **91**, 1-9.

Taketomi, T., Yoshiga, D., Taniguchi, K., Kobayashi, T., Nonami, A., Kato, R., Sasaki, A., Ishibashi, H., Moriyama, M., Nakamura, K. et al. (2005). Loss of mammalian Sprouty2 leads to enteric neuronal hyperplasia and esophageal achalasia. *Nat. Neurosci.* **8**, 855-857.

Tompers, D. M. and Labosky, P. A. (2004). Electroporation of murine embryonic stem cells: a step-by-step guide. *Stem Cells* **22**, 243-249.

Worl, J., Dutsch, F. and Neuhuber, W. L. (2002). Development of neuromuscular junctions in the mouse esophagus: focus on establishment and reduction of enteric co-innervation. *Anat. Embryol.* **205**, 141-152.

Yan, H., Bergner, A. J., Enomoto, H., Milbrandt, J., Newgreen, D. F. and Young, H. M. (2004). Neural cells in the esophagus respond to glial cell line-derived neurotrophic factor and neuturin, and are RET-dependent. *Dev. Biol.* **272**, 118-133.

Young, H. M., Hearn, C. J., Farlie, P. G., Canty, A. J., Thomas, P. Q. and Newgreen, D. F. (2001). GDNF is a chemoattractant for enteric neural cells. *Dev. Biol.* **229**, 503-516.